Theoretical Aspects of Neutrino Oscillations

PHY499
Undergraduate Thesis - 2024

Department of Physics
Shiv Nadar Institution of Eminence

Author:
Kaustubh Singh
(2010110343)

Under the guidance of **Dr. Kenji Nishiwaki**

Acknowledgements

I am grateful to Dr. Kenji Nishiwaki for his patience while dealing with me throughout the project.

I am also thankful to the department for having two semester long research project. It has taught me several valuable lessons.

Finally, I am grateful to my parents and friends who have helped me throughout despite a severe lack of credit.

Contents

Abstract

I start out by explaining the simplest model which describes the phenomenon of neutrino oscillations in free space.

After that, in my literature review I explain the techniques used to calculate transition probabilities for different neutrino states in the presence of a magnetic field, and apply those techniques to reproduce the results of the paper [4].

Then I move on to describing what Leggett-Garg inequalities are, and reproduce some results of a paper [10] which studies Leggett-Garg inequalities in the context of neutrino oscillations (in free space).

I then apply the formalism developed in [4] to successfully obtain violations of the Leggett-Garg inequalities when applied to neutrinos in the presence of a magnetic field.

Some curious features are observed, which lead to newer questions.

Chapter 1

Introduction

In this following chapter, I will present the most basic description of the phenomenon of neutrino oscillations using quantum mechanics. I will start by describing the phenomenon, then move on to showing the simplest model that features the same phenomenology and then use that model to perform some simple calculations.

1.1 Motivation and Model

In the standard model, neutrinos are spin half particles which only participate in weak interactions. There are three different types, or flavours of neutrinos: the electron neutrino, the muon neutrino and the tauon neutrino (corresponding to the leptons that accompany them in weak processes). Their corresponding symbols are ν_e, ν_μ and ν_τ respectively.

One would expect that an electron neutrino emitted at a point A, when detected at a separate point B to which it travelled would be detected as an electron neutrino. However, experiments like Homestake (1968) and Sudbury Neutrino Observatory (2002) found that the expected number of electron neutrinos coming from the Sun was lesser than what was theoretically predicted [1,2].

The simplest explanation for this discrepancy is that neutrinos change their flavour as they travel; so if an electron neutrino is emitted at point A, you might detect a muon or a tauon neutrino instead at B.

A model which describes this phenomenon can be constructed by assuming that a general neutrino flavour state is a superposition of three orthogonal base kets, $|\nu_e\rangle$, $|\nu_\mu\rangle$ and $|\nu_\tau\rangle$ in the Schrödinger picture:

$$|\nu(t)\rangle = \alpha_e(t)\,|\nu_e\rangle + \alpha_\mu(t)\,|\nu_\mu\rangle + \alpha_\tau(t)\,|\nu_\tau\rangle\,, \tag{1.1}$$

with $\langle\nu_\alpha|\nu_\beta\rangle = \delta_{\alpha\beta}$ where $\alpha, \beta \in \{e, \mu, \tau\}$. Flavour, just like spin, is an internal degree of freedom, so the general state of a neutrino particle can be expressed as a superposition of kets which are of the form $|\mathbf{p}\rangle \otimes |\nu_\alpha\rangle$, where $|\nu_\alpha\rangle \in \{\nu_e, \nu_\mu, \nu_\tau\}$ forms a basis for the flavour part of the state ket and $|\mathbf{p}\rangle$[1] forms a basis for the spatial part of the state ket.

Henceforth, Greek subscripts to the symbol ν will always take values from the set $\{e, \mu, \tau\}$. We are ignoring the spin degree of freedom and are assuming that the time-independent Hamiltonian $\hat{H}$ which governs the time evolution of $|\nu(t)\rangle$, has eigenkets with definite momentum (i.e. plane waves) and for a given momentum $\mathbf{p}$, has three orthogonal eigenkets $|\nu_i(\mathbf{p})\rangle = |\mathbf{p}\rangle \otimes |\nu_i\rangle =$

[1] $|\mathbf{p}\rangle$ is a momentum eignstate; $\hat{\mathbf{P}}\,|\mathbf{p}\rangle = \mathbf{p}\,|\mathbf{p}\rangle$

$|\mathbf{p}\rangle\,|\nu_i\rangle$ with $i \in \{1,2,3\}$ which have corresponding eigenvalues of the form $\sqrt{\mathbf{p}^2 + m_i^2}$, where the mass, m_i is in general different for the three states.

We have used the relativistic dispersion relation instead of the usual non-relativistic dispersion relation which naturally comes from the free Schrödinger equation because neutrinos, owing to their extremely low masses almost always travel at relativistic speeds. This requirement has been imposed in a slightly ad-hoc manner, and will be refined later when use the Dirac equation to describe the time evolution. The relativistic dispersion relation will arise naturally in that case.

If $|\nu_\alpha\rangle$ was a Hamiltonian eigenstate, we would not have the phenomenon of neutrino flavour changing during propagation[2]. To include this phenomenon, we are forced to conclude that the flavour eigenstates ($|\nu_e\rangle$, $|\nu_\mu\rangle$ and $|\nu_\tau\rangle$) are not stationary states and hence are not Hamiltonian eigenstates.

Hence the Hamiltonian eigenstates with momentum $\mathbf{p}$ have to be of the form $|\nu_i(\mathbf{p})\rangle := |\mathbf{p}\rangle \otimes |\nu_i\rangle = |\mathbf{p}\rangle\,|\nu_i\rangle$ with $i \in \{1,2,3\}$[3].

$$\hat{H}\,|\nu_i(\mathbf{p})\rangle = E_i(\mathbf{p})\,|\nu_i(\mathbf{p})\rangle \quad \text{with} \quad E_i(\mathbf{p}) = \sqrt{\mathbf{p}^2 + m_i^2}. \tag{1.2}$$

The base kets $|\nu_i\rangle$ with $i \in \{1,2,3\}$ are called *mass* eigenstates because they have a definite mass, as opposed the the flavour eigenstates which are a linear superposition of the mass eigenstates, so their mass is not fixed. Henceforth, Latin subscripts to the symbol ν will always take values from the set $\{1,2,3\}$. Additionally, $\langle\nu_i|\nu_j\rangle = \delta_{ij}$.

Since the eigenbasis for any Hamiltonian is always complete, the set of mass eigenstates must span the entire flavour Hilbert space. Since the flavour base kets and the mass base kets both form a orthogonal basis for the flavour Hilbert space, they must be related by a unitary matrix:

$$|\nu_\alpha\rangle = \sum_{i=1}^{3} \mathcal{U}^\dagger{}_{i\alpha}\,|\nu_i\rangle \quad \text{or} \quad \langle\nu_\alpha| = \sum_{i=1}^{3} \mathcal{U}_{\alpha i}\,\langle\nu_i|\,, \tag{1.3}$$

where $\mathcal{U}$ is a 3×3 unitary matrix (that is to say $\mathcal{U}_{\alpha i}\mathcal{U}^\dagger_{i\beta} = \delta_{\alpha\beta}$), called the PMNS (Pontecorvo–Maki–Nakagawa–Sakata) matrix. Since the basis elements are related by $\mathcal{U}^\dagger$, the components (or the wave-functions) would be related by $\mathcal{U}$, that is if $|\nu(t)\rangle = \alpha_e(t)\,|\nu_e\rangle + \alpha_\mu(t)\,|\nu_\mu\rangle + \alpha_\tau(t)\,|\nu_\tau\rangle = \alpha_1(t)\,|\nu_1\rangle + \alpha_2(t)\,|\nu_2\rangle + \alpha_3(t)\,|\nu_3\rangle$ then

$$\nu_\alpha(t) = \sum_{i=1}^{3} \mathcal{U}_{\alpha i}\nu_i(t). \tag{1.4}$$

The time evolution of a neutrino in an initial state $|\psi(t=0)\rangle = |\nu_i(\mathbf{p})\rangle = |\mathbf{p}\rangle\,|\nu_i\rangle$ would then be given by

$$|\psi(t)\rangle = \hat{U}(t,0)\,|\mathbf{p}\rangle\,|\nu_i\rangle = \exp(-i\hat{H}t)\,|\mathbf{p}\rangle\,|\nu_i\rangle = e^{-iE_i(\mathbf{p})t}\,|\mathbf{p}\rangle\,|\nu_i\rangle \tag{1.5}$$

Now that we have the time evolution of the energy eigenstates, we can calculate the time evolution of an arbitrary superposition of the energy eigenstates in a straightforward manner.

[2] Say for instance $|\nu_\alpha\rangle$ is a Hamiltonian eigenstate, and $|\nu(0)\rangle = |\nu_e\rangle$. Then $|\nu(t)\rangle = \hat{U}(t,0)\,|\nu_e\rangle = \exp(-i\hat{H}t)\,|\nu_e\rangle = \exp(-iE_e t)\,|\nu_e\rangle$. So the probability of finding the particle in the state ν_e after time t is $|\,\langle\nu(t)|\nu_e\rangle\,|^2 = 1$, which is not what we observe.

[3] Under our requirements, the Hamiltonian can be explicitly written as $\hat{H} = \sum_{i=1}^{3} \sqrt{m_i^2 + \hat{\mathbf{P}}^2} \otimes |\nu_i\rangle\,\langle\nu_i|$. Operator functions are defined as usual as $f(\hat{\mathbf{P}}) = \int d^3p f(\mathbf{p})\,|\mathbf{p}\rangle\,\langle\mathbf{p}|$.

1.2 Calculation of Transition Probabilities

Now we are going to use our model to calculate the transition probability of starting from an initial plane wave flavour eigenstate $|\nu_\alpha(\mathbf{p})\rangle := |\mathbf{p}\rangle\,|\nu_\alpha\rangle$ and ending up at a plane wave flavour eigenstate $|\nu_\beta(\mathbf{p}')\rangle := |\mathbf{p}'\rangle\,|\nu_\beta\rangle$ after travelling for a time t. Here, we have made the assumption that flavour eigenstates are composed of three mass eigenstates, each with *equal* momentum[4].

The transition probability is given by

$$\mathcal{P}_{\alpha\to\beta}(t) := |\mathcal{A}_{\alpha\to\beta}(t)|^2, \tag{1.6}$$

where the transition amplitude, $\mathcal{A}_{\alpha\to\beta}(t)$ is given by

$$\mathcal{A}_{\alpha\to\beta}(t) := \langle\nu_\beta(\mathbf{p}')|\hat{U}(t,0)|\nu_\alpha(\mathbf{p})\rangle\,. \tag{1.7}$$

Substituting (1.3) and (1.5) above,

$$\begin{aligned}
\mathcal{A}_{\alpha\to\beta}(t) &= \langle\nu_\beta(\mathbf{p}')|\hat{U}(t,0)|\nu_\alpha(\mathbf{p})\rangle \\
&= \sum_{i=1}^{3}\langle\nu_\beta(\mathbf{p}')|\,\hat{U}(t,0)\mathcal{U}^\dagger_{i\alpha}\,|\mathbf{p}\rangle\,|\nu_i\rangle \\
&= \sum_{i=1}^{3}\sum_{j=1}^{3}\mathcal{U}^\dagger_{i\alpha}\mathcal{U}_{\beta j}\,\langle\nu_j|\,\langle\mathbf{p}'|\,\hat{U}(t,0)\,|\mathbf{p}\rangle\,|\nu_i\rangle \\
&= \sum_{i=1}^{3}\sum_{j=1}^{3}\mathcal{U}^\dagger_{i\alpha}\mathcal{U}_{\beta j}e^{-iE_i(\mathbf{p})t}\,\langle\nu_j|\,\langle\mathbf{p}'|\mathbf{p}\rangle\,|\nu_i\rangle \\
&= \sum_{i=1}^{3}\sum_{j=1}^{3}\mathcal{U}^\dagger_{i\alpha}\mathcal{U}_{\beta j}e^{-iE_i(\mathbf{p})t}\delta^3(\mathbf{p}-\mathbf{p}')\delta_{ij} \\
&= \delta^3(\mathbf{p}-\mathbf{p}')\sum_{i=1}^{3}\mathcal{U}_{\beta i}e^{-iE_i(\mathbf{p})t}\mathcal{U}^\dagger_{i\alpha}.
\end{aligned} \tag{1.8}$$

The delta distribution above just enforces momentum conservation. We can drop that factor since we are interested only in the flavour transition probabilities.

In the high energy limit, we can approximate $E_i(\mathbf{p})$ as follows

$$\begin{aligned}
E_i(\mathbf{p}) &= \sqrt{\mathbf{p}^2+m_i^2} \\
&= |\mathbf{p}|\sqrt{1+\frac{m_i^2}{\mathbf{p}^2}} \\
&= |\mathbf{p}|\left(1+\frac{m_i^2}{2\mathbf{p}^2}\right)+\mathcal{O}\left(\frac{m_i^4}{2\mathbf{p}^4}\right).
\end{aligned} \tag{1.9}$$

Substituting this in (1.8) and dropping the delta distribution,

$$\mathcal{A}_{\alpha\to\beta}(t) = e^{-i|\mathbf{p}|t}\sum_{i=1}^{3}\mathcal{U}_{\beta i}\mathcal{U}^\dagger_{i\alpha}\exp\left(-i\frac{m_i^2}{2|\mathbf{p}|}t\right)+\mathcal{O}\left(\frac{m_i^4}{2\mathbf{p}^4}\right). \tag{1.10}$$

[4]The validation behind this assumption is non-trivial, and one needs to treat neutrinos as wave-packets to get a justification [3].

Then the oscillation probability in the high energy limit comes out to be:

$$\begin{aligned}\mathcal{P}_{\alpha\to\beta}(t) &= \left|\sum_{i=1}^{3}\mathcal{U}_{\beta i}\exp\left(-i\frac{m_i^2}{2|\mathbf{p}|}t\right)\mathcal{U}^{\dagger}_{i\alpha}\right|^2 + \mathcal{O}\left(\frac{m_i^4}{2\mathbf{p}^4}\right)\\ &\approx \left|\sum_{i=1}^{3}\mathcal{U}_{\beta i}\exp\left(-i\frac{\Delta m_{i1}^2}{2|\mathbf{p}|}t\right)\mathcal{U}^{\dagger}_{i\alpha}\right|^2,\end{aligned} \tag{1.11}$$

where $\Delta m_{i1}^2 := m_i^2 - m_1^2$. The transition probability depends on time through a periodic function, which is why these transition probabilities are called *oscillation* probabilities.

I will now show the oscillation probabilities explicitly, for the two flavour case.

1.3 Two Flavour Case

Assuming there are only two flavours base kets $|\nu_e\rangle$ and $|\nu_\mu\rangle$, the PMNS matrix will be a 2×2 unitary matrix. A 2×2 unitary matrix can be written in the form

$$\mathcal{U} = \begin{pmatrix}\cos\theta & \sin\theta\\ -\sin\theta & \cos\theta\end{pmatrix}. \tag{1.12}$$

Then by (1.3),

$$\begin{aligned}\langle\nu_e| &= \cos\theta\,\langle\nu_1| + \sin\theta\,\langle\nu_2|\,,\\ \langle\nu_\mu| &= -\sin\theta\,\langle\nu_1| + \cos\theta\,\langle\nu_2|\,.\end{aligned} \tag{1.13}$$

And the wave-functions as defined in (1.4),

$$\begin{aligned}\nu_e &= \nu_1\cos\theta + \nu_2\sin\theta,\\ \nu_\mu &= -\nu_1\sin\theta + \nu_2\cos\theta.\end{aligned} \tag{1.14}$$

Say at $t=0$, an electron neutrino is emitted ($|\nu(0)\rangle = |\nu_e\rangle$) as a plane wave with momentum $\mathbf{p}$. We are ignoring the momentum part of the state ket, since it is irrelevant in the final oscillation probability. Then the state ket at a later time t would be

$$|\nu(t)\rangle = \cos\theta e^{-iE_1t}\,|\nu_1\rangle + \sin\theta e^{-iE_2t}\,|\nu_2\rangle \tag{1.15}$$

Where $E_1 = E_1(\mathbf{p})$ and $E_2 = E_2(\mathbf{p})$ are as given in (1.9).

Then the oscillation amplitude $\mathcal{P}_{e\to\mu}$ would be given by

$$\begin{aligned}\mathcal{P}_{e\to\mu}(t) &= |\,\langle\nu_\mu|\nu_e(t)\rangle\,|^2\\ &= |(-\sin\theta\,\langle\nu_1| + \cos\theta\,\langle\nu_2|)(\cos\theta e^{-iE_1t}\,|\nu_1\rangle + \sin\theta e^{-iE_2t}\,|\nu_2\rangle)|^2\\ &= \sin^2\theta\cos^2\theta|(e^{-iE_1t} - e^{-iE_2t})|^2\\ &= \frac{1}{4}\sin^2 2\theta[(\cos E_1t - \cos E_2t)^2 + (\sin E_1t - \sin E_2t)^2]\\ &= \frac{1}{4}\sin^2 2[2 - 2(\cos E_1t\cos E_2t + \sin E_1t\sin E_2t)]\\ &= \frac{1}{2}\sin^2 2\theta[1-\cos(E_1-E_2)t]\\ &= \sin^2 2\theta\sin^2\left[\frac{(E_1-E_2)t}{2}\right].\end{aligned} \tag{1.16}$$

Substituting (1.9) above, we get

$$\mathcal{P}_{e\to\mu}(t) = \sin^2 2\theta \sin^2\left(\frac{\Delta m_{12}^2 t}{4|\mathbf{p}|}\right). \tag{1.17}$$

It can similarly be shown that

$$\mathcal{P}_{e\to e}(t) = 1 - \sin^2 2\theta \sin^2\left(\frac{\Delta m_{12}^2 t}{4|\mathbf{p}|}\right) = \mathcal{P}_{\mu\to\mu}(t). \tag{1.18}$$

We can also show that $\mathcal{P}_{e\to\mu}(t) = \mathcal{P}_{\mu\to e}(t)$.

Chapter 2

Literature Review

2.1 Neutrino Oscillations in the Presence of a Magnetic Field

Here, I will outline the technique developed in [4]. They consider two flavour neutrino oscillations in the presence of an external magnetic field.

2.1.1 Describing the Hamiltonian

We begin by assuming that the dynamics of a neutrino wave-function in a magnetic field is described by the Dirac equation's single particle interpretation:

$$(\gamma_\mu p^\mu - m_i - \mu_i \boldsymbol{\Sigma} \cdot \mathbf{B})\nu_i(p) = 0. \tag{2.1}$$

Above, $\nu_i(p)$ is the neutrino wave-function, $\mathbf{B}$ is the magnetic field, p^μ is the momentum four-vector, m_i is the mass of the i^{th} mass eigenstate, μ_i is the magnetic moment of the i^{th} mass eigenstate and

$$\Sigma_i = \begin{pmatrix} \sigma_i & 0 \\ 0 & \sigma_i \end{pmatrix}$$

is the spin operator (σ_i is the i^{th} Pauli matrix) We can rewrite the above equation and recast it in the form of the time independent Schrödinger equation.

$$\begin{aligned}
(\gamma_\mu p^\mu - m_i - \mu_i \boldsymbol{\Sigma} \cdot \mathbf{B})\nu_i(p) &= 0, & (2.2)\\
(E\gamma_0 - \boldsymbol{\gamma} \cdot \mathbf{p} - m_i - \mu_i \boldsymbol{\Sigma} \cdot \mathbf{B})\nu_i(p) &= 0, & (2.3)\\
E\nu_i(p) &= (\boldsymbol{\gamma} \cdot \mathbf{p} + m_i + \mu_i \boldsymbol{\Sigma} \cdot \mathbf{B})\nu_i(p), & (2.4)\\
\hat{H}\nu_i(p) &= E\nu_i(p). & (2.5)
\end{aligned}$$

Hence the Hamiltonian is

$$\hat{H}_i = \boldsymbol{\gamma} \cdot \mathbf{p} + m_i + \mu_i \boldsymbol{\Sigma} \cdot \mathbf{B}. \tag{2.6}$$

In the paper [4], they take this Hamiltonian and use it to get the energy eigenvalues as

$$E_i^{\pm} = \sqrt{m_i^2 + p^2 + {\mu_i}^2\mathbf{B}^2 \pm 2\mu_i\sqrt{m_i^2\mathbf{B}^2 + \mathbf{p}^2\mathbf{B}^2 - (\mathbf{p} \cdot \mathbf{B})^2}}, \tag{2.7}$$

Henceforth, we will restrict ourselves to the the case when $\mathbf{B} = (B_\perp, 0, B_\parallel)$ and $\mathbf{p} = (0, 0, p)$. Here $B_\perp$ is the component of the magnetic field that is perpendicular to the direction of propagation and $B_\parallel$ is the component of the magnetic field that is parallel to the direction of propagation.

This is valid since we can always reorient our axes since the Dirac equation is covariant under Lorentz transformations (which includes rotations). In this case,

$$E_i^{\pm} = \sqrt{m_i^2 + p^2 + {\mu_i}^2\mathbf{B}^2 \pm 2\mu_i\sqrt{m_i^2\mathbf{B}^2 + p^2 B_\perp^2}}. \tag{2.8}$$

In the high energy limit and weak magnetic moment limit, we make the following assumptions: $p \gg m_i \gg \mu_i|\mathbf{B}|$ for $i \in \{1, 2\}$. In this limit,

$$\begin{aligned} E_i^{\pm} &= \sqrt{m_i^2 + p^2 + {\mu_i}^2\mathbf{B}^2 \pm 2\mu_i\sqrt{m_i^2\mathbf{B}^2 + p^2 B_\perp^2}} \\ &\approx \sqrt{m_i^2 + p^2 + {\mu_i}^2\mathbf{B}^2 \pm 2\mu_i p B_\perp} \\ &\approx p\left(1 + \frac{m_i^2}{2p^2} + \frac{\mu_i^2\mathbf{B}^2}{2p^2} \pm \frac{\mu_i B_\perp}{p}\right) \\ &\approx p + \frac{m_i^2}{2p} + \pm\mu_i B_\perp. \end{aligned} \tag{2.9}$$

Note that we have removed the negative energy solutions by hand. Also note that it is only that component of the magnetic field which is perpendicular to the direction of propagation, that affects the energy spectrum in our limiting case.

2.1.2 Finding the Stationary States

The observable orthogonal states are the flavour eigenstates and the helicity[1] eigenstates. Note that in the high energy limit, chirality[2] and helicity eigenstates are the same[3] [5], so in that limit, one can talk about helicity and chirality interchangeably for particles. The basis states then are $|\nu_e^L\rangle, |\nu_e^R\rangle, |\nu_\mu^L\rangle$ and $|\nu_\mu^R\rangle$.

However, as we had established in the last section, the flavour eigenstates are not stationary states. The wave-functions in the flavour and the mass eigenbasis are related by:

$$\begin{aligned} \nu_e^{L(R)} &= \nu_1^{L(R)}\cos\theta + \nu_2^{L(R)}\sin\theta, \\ \nu_\mu^{L(R)} &= -\nu_1^{L(R)}\sin\theta + \nu_2^{L(R)}\cos\theta. \end{aligned} \tag{2.10}$$

Additionally, note that the helicity operator commutes with the Dirac Hamiltonian when there is no magnetic field, so the helicity eigenstates states are stationary states (just like how flavour eigenstates are stationary states when the mixing angle, θ is zero).

However, in the presence of a non-zero magnetic field, the helicity operator does not commute with the Dirac Hamiltonian, so we must find a different set of basis states which would be the Dirac Hamiltonian's (2.6) eigenstates and then express the helicity states as a superposition of those states (just like how we express the flavour eigenstates as a linear superposition of the mass eigenstates which are the Hamiltonian eigenstates).

Since the helicity operator does not commute with the Hamiltonian in (2.6) for non-zero magnetic fields, the helicity eigenstates ($|\nu_i^L\rangle, |\nu_i^R\rangle$) are not stationary states. They would also oscillate (just like how flavour states are not stationary states and oscillate for non-zero mixing angle θ). So in addition to flavour oscillations $\nu_e^L \leftrightarrow \nu_\mu^L$ we would also observe spin oscillations $\nu_e^L \leftrightarrow \nu_e^R$ and spin-flavour oscillations $\nu_e^L \leftrightarrow \nu_\mu^R$.

[1] The helicity operator is defined as $\hat{h} = \mathbf{p}\cdot\mathbf{\Sigma}/2$ [5].
[2] The chirality operator is defined as $\gamma^5 = i\gamma^0\gamma^1\gamma^2\gamma^3$ [5].
[3] This is true for particles. For anti-particles, an additional minus sign comes

One could try and attempt a brute force solution, as is done in [6], but it is quiet cumbersome even when one uses symbolic manipulators. The authors of [4] came up with an ingenious (albeit unmotivated) solution which allows us to calculate the oscillation probability.

They define a new operator $\hat{S}_i$ as:

$$\hat{S}_i = \frac{1}{N_i}\left[\mathbf{\Sigma}\cdot\mathbf{B} - \frac{i}{m_i}\gamma_0\gamma_5[\mathbf{\Sigma}\times\mathbf{p}]\cdot\mathbf{B}\right], \tag{2.11}$$

where

$$\frac{1}{N_i} = \frac{m_i}{\sqrt{m_i^2\mathbf{B}^2 + \mathbf{p}^2 B_\perp^2}}. \tag{2.12}$$

It can be shown that the $\hat{S}_i$ operator commutes with the Dirac Hamiltonian for the corresponding mass eigenstate in (2.6):

$$[\hat{S}_i, \hat{H}_i] = 0. \tag{2.13}$$

I used Python's symbolic manipulator (the sympy library) to confirm this. Due to this property, $\hat{S}_i$ and the Hamiltonian can have simultaneous eigenstates.

Additionally, the $\hat{S}_i$ operator can be shown to be Hermitian and have eigenvalues ± 1. This also was checked using sympy.

Let $|\nu_i^\pm\rangle$ be the eigenstates of $\hat{S}_i$. Then:

$$\hat{S}_i\,|\nu_i^\pm\rangle = \pm\,|\nu_i^\pm\rangle\,. \tag{2.14}$$

With

$$\langle\nu_i^s|\nu_k^{s'}\rangle = \delta_{ik}\delta_{ss'}, \quad \text{where} \quad s, s' \in \{+,-\}. \tag{2.15}$$

Since $\hat{S}_i$ has eigenvalues ± 1, we can construct the projection operators which project a ket onto the ± 1 eigenspace in quiet a straightforward manner:

Let the projection operator onto the $+(-)$ eigenspace be $\hat{P}_{i+}(\hat{P}_{i-})$. Then, the spectral decomposition of $\hat{S}_i$ is:

$$\hat{S}_i = \hat{P}_{i+} - \hat{P}_{i-} \tag{2.16}$$

Also, since $\hat{S}_i$ is Hermitian, it will have a complete set of eigenvectors, which means that $\hat{P}_{i+} + \hat{P}_{i-} = I$, I being the identity operator. We can solve for the projection operators by adding and subtracting these two equations:

$$\hat{P}_{i\pm} = \frac{1 \pm \hat{S}_i}{2}. \tag{2.17}$$

Now we can expand the helicity eigenfunctions in terms of the $\hat{S}_i$ eigenfunctions as follows:

$$\nu_i^L(t) = c_i^+\nu_i^+(t) + c_i^-\nu_i^-(t), \tag{2.18}$$
$$\nu_i^R(t) = d_i^+\nu_i^+(t) + d_i^-\nu_i^-(t). \tag{2.19}$$

This can be equivalently written as

$$\begin{pmatrix}\nu_i^L(t)\\ \nu_i^R(t)\end{pmatrix} = \begin{pmatrix}c_i^+ & c_i^-\\ d_i^+ & d_i^-\end{pmatrix}\begin{pmatrix}\nu_i^+(t)\\ \nu_i^-(t)\end{pmatrix}, \tag{2.20}$$

which is analogous to how one expands the flavour eigenstates (non-stationary states) in terms of the mass eigenstates (stationray) states via a matrix (the PMNS matrix).

The time independent coefficients $c_i^{\pm}$ and $d_i^{\pm}$ depend only on the initial conditions of the neutrino state. We can not determine what these coefficients are directly, but it is straightforward to find the quadratic combinations $|c_i^{\pm}|^2$, $|d_i^{\pm}|^2$ and $(d_i^{\pm})^* c_i^{\pm}$, once we fix the initial conditions. Fortunately, it is only these quadratic combinations which appear in oscillation probability calculations.

First note that

$$\langle \nu_k^{s'} | \hat{P}_i^s | \nu_i^s \rangle = \delta_{ik}\delta_{ss'} \quad \text{where} \quad s, s' \in \{+, -\}. \tag{2.21}$$

Which follows from (2.15). Then by direct substitution of (2.18) and (2.19) and using the above orthogonalization condition, it can be shown that

$$|c_i^{\pm}|^2 = \langle \nu_i^L | \hat{P}_i^{\pm} | \nu_i^L \rangle , \tag{2.22}$$

$$|d_i^{\pm}|^2 = \langle \nu_i^R | \hat{P}_i^{\pm} | \nu_i^R \rangle , \tag{2.23}$$

$$(d_i^{\pm})^* c_i^{\pm} = \langle \nu_i^R | P_i^{\pm} | \nu_i^L \rangle . \tag{2.24}$$

We know the form of $\hat{P}_{i\pm}$ from (2.17). We can take the initial conditions to be

$$\nu_i^L(0) = \frac{1}{\sqrt{2}} \begin{pmatrix} 0 \\ -1 \\ 0 \\ 1 \end{pmatrix}, \quad \nu_i^R(0) = \frac{1}{\sqrt{2}} \begin{pmatrix} 1 \\ 0 \\ 1 \\ 0 \end{pmatrix}, \tag{2.25}$$

as they correspond to -1 and +1 chirality eigenkets in the Pauli-Dirac representation. Neutrinos, due to their small masses always travel at ultra-relativistic speeds, the high energy approximation is valid. In that limit, chirality and helicity states are the same, so it is justified to equate helicity eigenstates to chirality eigenstates.

Substituting (2.25) and (2.17) into (2.22), (2.23) and (2.24), I calculated the quadratic combinations and got:

$$|c_i^{\pm}|^2 = \frac{1}{2}\left(1 \mp \frac{m_i B_{\parallel}}{\sqrt{m_i^2 B^2 + p^2 B_{\perp}^2}}\right), \tag{2.26}$$

$$|d_i^{\pm}|^2 = \frac{1}{2}\left(1 \pm \frac{m_i B_{\parallel}}{\sqrt{m_i^2 B^2 + p^2 B_{\perp}^2}}\right), \tag{2.27}$$

$$(d_i^{\pm})^* c_i^{\pm} = \mp \frac{1}{2} \frac{p B_{\perp}}{\sqrt{m_i^2 B^2 + p^2 B_{\perp}^2}}. \tag{2.28}$$

In their paper [4], the signs in red were flipped; $\pm \to \mp$ and $\mp \to \pm$.

2.1.3 Time Evolution

Say $|\psi(0)\rangle = |\nu_i^L\rangle = c_1^+ |\nu_1^+\rangle + c_1^- |\nu_1^-\rangle$. Then,

$$|\psi(t)\rangle = |\nu_i^L(t)\rangle = c_1^+ e^{-iE_1^+ t} |\nu_1^+\rangle + c_1^- e^{-iE_1^- t} |\nu_1^-\rangle . \tag{2.29}$$

Similarly, if $|\psi(0)\rangle = |\nu_i^R\rangle = d_1^+ |\nu_1^+\rangle + d_1^- |\nu_1^-\rangle$. Then,

$$|\psi(t)\rangle = |\nu_i^R(t)\rangle = d_1^+ e^{-iE_1^+ t} |\nu_1^+\rangle + d_1^- e^{-iE_1^- t} |\nu_1^-\rangle . \tag{2.30}$$

Now say $|\psi(0)\rangle = |\nu_e^L\rangle = \cos\theta\,|\nu_1^L\rangle + \sin\theta\,|\nu_2^L\rangle$. Then,

$$|\psi(t)\rangle = |\nu_e^L(t)\rangle = \cos\theta\,|\nu_1^L(t)\rangle + \sin\theta\,|\nu_2^L(t)\rangle\,. \tag{2.31}$$

This implies

$$\begin{aligned}|\nu_e^L(t)\rangle = &\left(c_1^+ e^{-iE_1^+ t}\,|\nu_1^+\rangle + c_1^- e^{-iE_1^- t}\,|\nu_1^-\rangle\right)\cos\theta \\ &+ \left(c_2^+ e^{-iE_2^+ t}\,|\nu_2^+\rangle + c_2^- e^{-iE_2^- t}\,|\nu_2^-\rangle\right)\sin\theta.\end{aligned} \tag{2.32}$$

Similarly it can be shown that

$$\begin{aligned}|\nu_\mu^L(t)\rangle = &-\left(c_1^+ e^{-iE_1^+ t}\,|\nu_1^+\rangle + c_1^- e^{-iE_1^- t}\,|\nu_1^-\rangle\right)\sin\theta \\ &+ \left(c_2^+ e^{-iE_2^+ t}\,|\nu_2^+\rangle + c_2^- e^{-iE_2^- t}\,|\nu_2^-\rangle\right)\cos\theta,\end{aligned} \tag{2.33}$$

$$\begin{aligned}|\nu_e^R(t)\rangle = &\left(d_1^+ e^{-iE_1^+ t}\,|\nu_1^+\rangle + d_1^- e^{-iE_1^- t}\,|\nu_1^-\rangle\right)\cos\theta \\ &+ \left(d_2^+ e^{-iE_2^+ t}\,|\nu_2^+\rangle + d_2^- e^{-iE_2^- t}\,|\nu_2^-\rangle\right)\sin\theta,\end{aligned} \tag{2.34}$$

$$\begin{aligned}|\nu_\mu^R(t)\rangle = &-\left(d_1^+ e^{-iE_1^+ t}\,|\nu_1^+\rangle + d_1^- e^{-iE_1^- t}\,|\nu_1^-\rangle\right)\sin\theta \\ &+ \left(d_2^+ e^{-iE_2^+ t}\,|\nu_2^+\rangle + d_2^- e^{-iE_2^- t}\,|\nu_2^-\rangle\right)\cos\theta.\end{aligned} \tag{2.35}$$

2.1.4 Calculation of Oscillation Probabilities

In order to calculate the oscillation amplitudes, we will require the quadratic combinations in (2.26), (2.27) and (2.28). In the high energy limit, when $p \gg m_i \gg \mu_i|\mathbf{B}|$, the quadratic combinations reduce to:

$$|c_i^\pm|^2 = |d_i^\pm|^2 = \frac{1}{2} \quad \text{and} \quad (d_i^\pm)^* c_i^\pm = \mp\frac{1}{2}. \tag{2.36}$$

Now we can calculate the oscillation probabilities.

First we define

$$\mu_\pm = \frac{\mu_1 \pm \mu_2}{2}, \tag{2.37}$$

and

$$\Delta m^2 = m_2^2 - m_1^2. \tag{2.38}$$

Flavour Oscillation $\nu_e^L \to \nu_\mu^L$

$$\begin{aligned}
\mathcal{P}_{\nu_e^L \to \nu_\mu^L}(t) &= |\langle \nu_\mu^L(0)|\nu_e^L(t)\rangle|^2 \\
&= \sin^2\theta\cos^2\theta\Big| - |c_1^+|^2 e^{-iE_1^+ t} - |c_1^-|^2 e^{-iE_1^- t} + |c_2^+|^2 e^{-iE_2^+ t} + |c_2^-|^2 e^{-iE_2^- t}\Big|^2 \\
&= \frac{1}{4}\sin^2\theta\cos^2\theta\Big| - e^{-iE_1^+ t} - e^{-iE_1^- t} + e^{-iE_2^+ t} + e^{-iE_2^- t}\Big|^2 \quad \text{after substituting (2.36)} \\
&= \frac{1}{4}\sin^2\theta\cos^2\theta\Big| - e^{\frac{-im_1^2 t}{2p}}(e^{-i\mu_1 B_\perp t} + e^{i\mu_1 B_\perp t}) + e^{\frac{-im_2^2 t}{2p}}(e^{-i\mu_2 B_\perp t} + e^{i\mu_2 B_\perp t})\Big|^2 \quad \text{substituting (2.9)} \\
&= \frac{\sin^2 2\theta}{4}\Big| - e^{\frac{-i\Delta m^2 t}{2p}}\cos(\mu_1 B_\perp t) + \sin(\mu_2 B_\perp t)\Big|^2 \\
&= \frac{\sin^2 2\theta}{4}\left[\cos^2(\mu_1 B_\perp t) + \cos^2(\mu_2 B_\perp t) - 2\cos(\mu_2 B_\perp t)\cos(\mu_1 B_\perp t)\cos\left(\frac{\Delta m^2 t}{2p}\right)\right] \\
&= \frac{\sin^2 2\theta}{4}\left[(\cos^2(\mu_1 B_\perp t) - \cos^2(\mu_2 B_\perp t))^2 + 2\cos(\mu_2 B_\perp t)\cos(\mu_1 B_\perp t)\left[1 - \cos\left(\frac{\Delta m^2 t}{2p}\right)\right]\right] \\
&= \frac{\sin^2 2\theta}{4}\left[(\cos(\mu_1 B_\perp t) - \cos(\mu_2 B_\perp t))^2 + 2\cos(\mu_2 B_\perp t)\cos(\mu_1 B_\perp t)\left[1 - \cos\left(\frac{\Delta m^2 t}{2p}\right)\right]\right], \\
\mathcal{P}_{\nu_e^L \to \nu_\mu^L}(t) &= \sin^2 2\theta\left[\sin^2(\mu_+ B_\perp t)\sin^2(\mu_- B_\perp t) + \cos(\mu_2 B_\perp t)\cos(\mu_1 B_\perp t)\sin^2\left(\frac{\Delta m^2 t}{4p}\right)\right].
\end{aligned} \tag{2.39}$$

Helicity Oscillation $\nu_e^L \to \nu_e^R$

$$\begin{aligned}
\mathcal{P}_{\nu_e^L \to \nu_e^R}(t) &= |\langle \nu_e^R(0)|\nu_e^L(t)\rangle|^2 \\
,\mathcal{P}_{\nu_e^L \to \nu_e^R}(t) &= \Big\{\sin(\mu_+ B_\perp t)\cos(\mu_- B_\perp t) + \cos 2\theta \sin(\mu_- B_\perp t)\cos(\mu_+ B_\perp t)\Big\}^2 \\
&\quad - \sin^2 2\theta \sin(\mu_1 B_\perp t)\sin(\mu_2 B_\perp t)\sin^2\left(\frac{\Delta m^2}{4p}t\right).
\end{aligned} \tag{2.40}$$

Helicity and Flavour Oscillation $\nu_e^L \to \nu_\mu^R$

$$\begin{aligned}
\mathcal{P}_{\nu_e^L \to \nu_\mu^R}(t) &= |\langle \nu_\mu^R(0)|\nu_e^L(t)\rangle|^2, \\
\mathcal{P}_{\nu_e^L \to \nu_\mu^R}(t) &= \sin^2 2\theta\Big\{\sin^2(\mu_- B_\perp t)\cos^2(\mu_+ B_\perp t) + \sin(\mu_1 B_\perp t)\sin(\mu_2 B_\perp t)\sin^2\frac{\Delta m^2}{4p}t\Big\}.
\end{aligned} \tag{2.41}$$

Survival Probability $\nu_e^L \to \nu_e^L$

$$\begin{aligned}
\mathcal{P}_{\nu_e^L \to \nu_e^L}(t) &= |\langle \nu_e^L(0)|\nu_e^L(t)\rangle|^2, \\
\mathcal{P}_{\nu_e^L \to \nu_e^L}(t) &= \Big\{\cos(\mu_+ B_\perp t)\cos(\mu_- B_\perp t) - \cos 2\theta \sin(\mu_+ B_\perp t)\sin(\mu_- B_\perp t)\Big\}^2 \\
&\quad - \sin^2 2\theta \cos(\mu_1 B_\perp t)\cos(\mu_2 B_\perp t)\sin^2\left(\frac{\Delta m^2}{4p}t\right).
\end{aligned} \tag{2.42}$$

The rest of the transition probabilities can be calculated similarly, and the calculations have been shown in A

2.1.5 Plots of Oscillation Probabilities

Using the transition amplitudes that were calculated, I plotted the graph the authors of [4] showed in their paper.

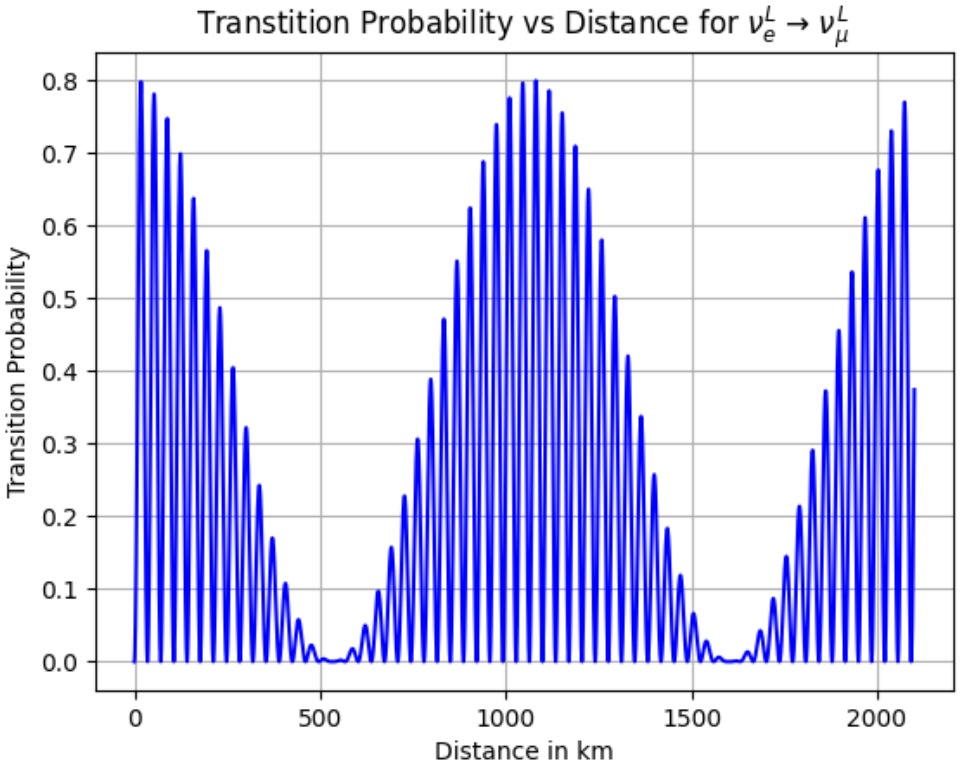

Figure 1 Plot of $\nu_e^L \to \nu_\mu^L$ transition amplitude as a function of distance. $L = ct$ in the ultra-relativistic limit. Here I took $p = 1$ MeV, $\mu_1 = \mu_2 = \mu_B \times 10^{-20}$, $B_\perp = 10^{12}$ T, $\Delta m^2 = 7 \times 10^{-5}$ eV^2 and $\sin^2 2\theta = 0.8$.

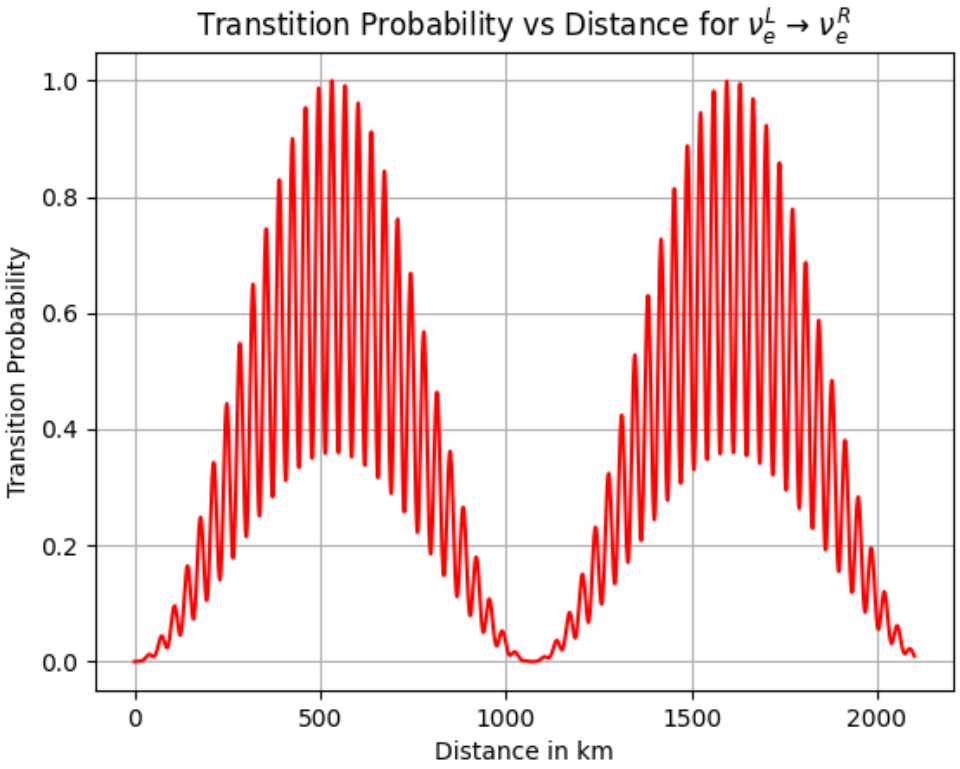

Figure 2 Plot of $\nu_e^L \to \nu_e^R$ transition amplitudes as a function of distance. $L = ct$ in the ultra-relativistic limit. Here I took $p = 1$ MeV, $\mu_1 = \mu_2 = \mu_B \times 10^{-20}$, $B_\perp = 10^{12}$ T, $\Delta m^2 = 7 \times 10^{-5}$ eV^2 and $\sin^2 2\theta = 0.8$.

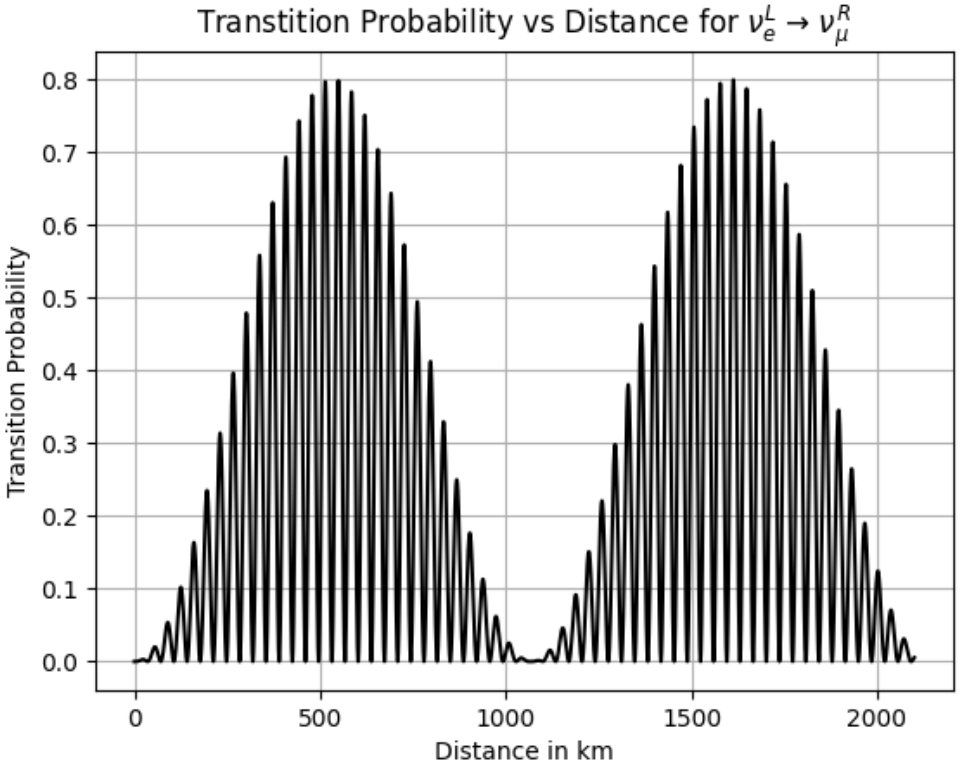

Figure 3 Plot of $\nu_e^L \to \nu_\mu^R$ transition amplitudes as a function of distance. $L = ct$ in the ultra-relativistic limit. Here I took $p = 1$ MeV, $\mu_1 = \mu_2 = \mu_B \times 10^{-20}$, $B_\perp = 10^{12}$ T, $\Delta m^2 = 7 \times 10^{-5}$ eV^2 and $\sin^2 2\theta = 0.8$.

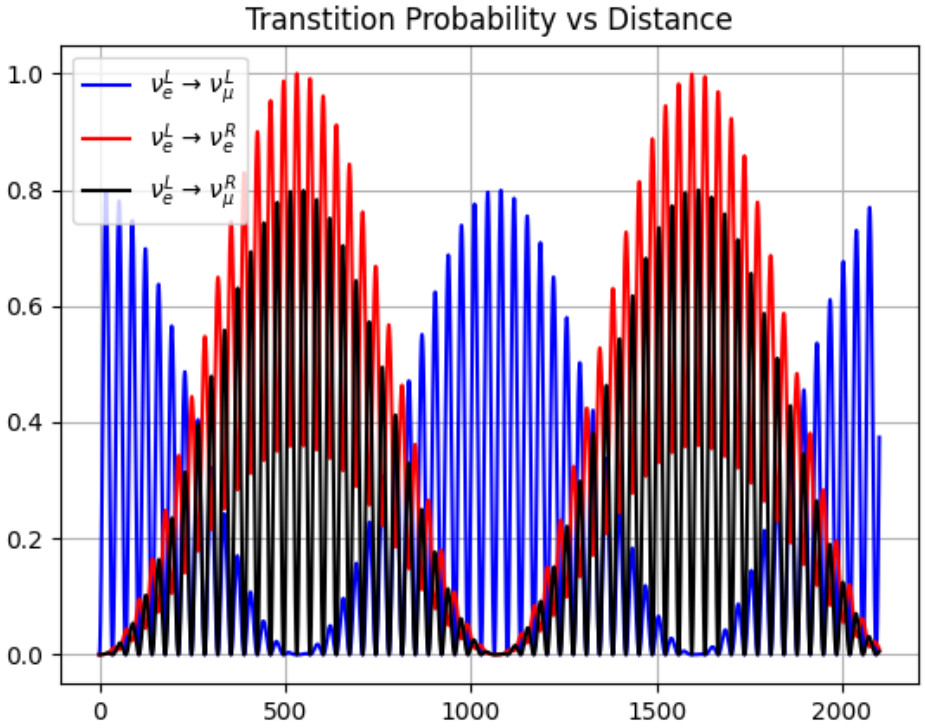

Figure 4 Plot of all the transition amplitudes as a function of distance. $L = ct$ in the ultra-relativistic limit. Here I took $p = 1$ MeV, $\mu_1 = \mu_2 = \mu_B \times 10^{-20}$, $B_\perp = 10^{12}$ T, $\Delta m^2 = 7 \times 10^{-5}$ eV^2 and $\sin^2 2\theta = 0.8$.

The higher frequency oscillations are oscillations coming from the standard oscillation phase of $\Delta m^2/4pt$, which are enveloped by a lower frequency curve which comes from the perpendicular magnetic field.

2.2 Leggett-Garg Inequalities

Leggett-Garg inequalities, like the Bell's inequalities are a set of inequalities which hold for a classical or macroscopic system[4], but are violated by quantum systems. This highlights how our classical intuitions fail to hold for quantum systems.

The Legget-Garg inequalities are analogous to Bell's[5] inequalities. The difference is that the CHSH inequality involves space-like separated measurements, while the Leggett-Garg inequality is derived for time-like separated measurements.

Here, I will provide a brief overview of the Leggett-Garg inequalities, explain how Legget and Garg [8] codified classicity, and then provide a derivation of the Legget-Garg inequalities (LGIs) based on the requirements imposed on a classical system. I will then move on to LGI violations by neutrinos.

[4]What Leggett and Garg meant by a classical or macroscopic system will be made precise soon.

[5]Bell's inequalities are used as an umbrella term for several inequalities of a similar nature. When I mention Bell's inequlities, I will be talking about the CHSH inequality [7]

2.2.1 Codification of Classicity

Before we arrive at the inequalities, we must first define what it means for a system to be classical or macroscopic. The conditions which Leggett and Garg required a system to have in order for it to be classical can be codified in two assumptions:

- **Macroscopic Realism (MR)** : The *state* of a system is defined by an ordered set of *observables*. At all times, the system will be in one of these states.
- **Non Invasive Measurements (NIM)** : it is possible to measure the state of a system with an arbitrarily small perturbation to its subsequent dynamics.

Leggett-Garg inequalities, like the CHSH inequality are derived by building upon notions of how we expect a classical system to behave. It is not a result about quantum mechanics.

Note that these assumptions do not require the system to be deterministic.

So by macroscopic realism, the state of a "classical" system, will take values from the set $\mathcal{S} = \{(O_1, O_2, \ldots, O_N) : O_k \in \mathcal{V}_k\} = \mathcal{V}_1 \times \mathcal{V}_2 \times \cdots \times \mathcal{V}_N$, where O_k is a certain observable which can takes values from the set $\mathcal{V}_k$.

For instance, think of a coin, which can either by in the heads states ($\uparrow$) or tails state ($\downarrow$), and additionally can either be blue or red.

For this system, the *observables* are the spin $\mathcal{V}_{\text{spin}} = \{\uparrow, \downarrow\}$ and colour $\mathcal{V}_{\text{colour}} = \{\text{red}, \text{blue}\}$.

Then a possible *state* of this system can be $(\uparrow, \text{red})$, corresponding to $\uparrow$.

The salient feature of macroscopic realism is that states are defined only by observables; right before a measurement, the system is in a state defined by some observables which are some physical properties of the system which can be determined experimentally, and upon making a measurement you would find said observables to correspond to what the state of the system was before the measurement was made.

Note that this requirement is completely contrary to what one expects from a quantum system. For a quantum system, the set of observables would be the complete set of commuting observables (CSCOs), whose eigenvalues form the orderd sets which are observed in experiments.

A quantum state however, is defined as an element of a Hilbert space in which the orthogonal simultaneous eigenkets of the CSCOs would correspond to a definite set of observables, but one can have linear superposition of these eigenkets which do not correspond to a definite set of observables.

In our example, a quantum system can have state like $(|\uparrow\rangle + |\downarrow\rangle)/\sqrt{2}$ in addition to states like $|\uparrow\rangle$. While the latter state corresponds to two fixed observables, whereas the former state does not correspond to any fixed observables.

Analogous to how locality is used in CHSH to prevent one measurement from affecting another spatially measurement, the non invasive postulate is used in LGIs to prevent one measurement from affecting the other.

2.2.2 Proof of the Leggett-Garg Inequalities

I will outline the proof in [9].

Say we have a classical system, which obeys MR and NIM. Additionally, say there is a dichotomous observable Q (it takes values ± 1) which is defined for this system. The value that this observable takes will be dependent on time t, as the system evolves with time.

Further assume that we do not know the initial state of the system, so we do not know the value of Q at any given time.

Say we measure Q at three time stamps t_1, t_2 and t_3, and label the outcome Q_1, Q_2 and Q_3 respectively. Since we do not know what these values could be, we can treat them as random variables.

Then the macroscopic realism and non invasive measurement properties imply that there exists a joint probability distribution function $\mathbf{P}(Q_1 = s_1, Q_2 = s_2, Q_3 = s_3)$, which would tell us the probability of finding the Q_1 to be measured as s_1, Q_2 to be measured as s_2 and Q_3 to be measured as s_3 [9].

Now we define the *two time correlation function*, C_{12} as:

$$C_{12} := \sum_{s_1,s_2,s_3=\pm 1} s_1 s_2 \mathbf{P}(Q_1 = s_1, Q_2 = s_2, Q_3 = s_3) = \mathbf{E}[Q_1 Q_2]. \tag{2.43}$$

Similarly we can define C_{23} and C_{13}:

$$C_{23} := \sum_{s_1,s_2,s_3=\pm 1} s_2 s_3 \mathbf{P}(Q_1 = s_1, Q_2 = s_2, Q_3 = s_3) = \mathbf{E}[Q_1 Q_2]. \tag{2.44}$$

$$C_{31} := \sum_{s_1,s_2,s_3=\pm 1} s_3 s_1 \mathbf{P}(Q_1 = s_1, Q_2 = s_2, Q_3 = s_3) = \mathbf{E}[Q_1 Q_2]. \tag{2.45}$$

Now we define a Legget-Garg parameter,K_3:

$$K_3 = C_{12} + C_{23} - C_{31} \tag{2.46}$$

Now substituting the definitions (2.43), (2.44) and (2.45) in (2.46) and using completeness:

$$\sum_{s_1,s_2,s_3=\pm 1} \mathbf{P}(Q_1 = s_1, Q_2 = s_2, Q_3 = s_3) = 1, \tag{2.47}$$

we get

$$K_3 = 1 - 4[\mathbf{P}(+,-,+) + \mathbf{P}(-,+,-)]. \tag{2.48}$$

I am using the notation where $\mathbf{P}(+,-,+) := \mathbf{P}(+1,-1,+1)$.

Since $0 \leq \mathbf{P}(+,-,+) \leq 1$ and $0 \leq \mathbf{P}(-,+,-) \leq 1$, we can get the upper bounds on K_3 by setting $\mathbf{P}(+,-,+) = \mathbf{P}(-,+,-) = 0$ which gives a value of $K_3 = 1$, and the lower bound by setting $\mathbf{P}(+,-,+) + \mathbf{P}(-,+,-) = 1$, which yields the lower bound of -3.

$$-3 \leq K_3 \leq 1. \tag{2.49}$$

Similarly, we can measure Q at n instances and define n two-time correlation functions C_{12}, C_{23},...,$C_{n-1,n}$ and $C_{n,1}$, and then define

$$K_n = -C_{n,1} + \sum_{i=1}^{n-1} C_{i,i+1}, \tag{2.50}$$

and corresponding bounds on K_n can be calculated [9] as:

$$\begin{aligned} -n \leq K_n \leq n-2 \qquad & n \geq 3, \text{ odd}, \\ -(n-2) \leq K_n \leq n-2 \quad & n \geq 4, \text{ even}. \end{aligned} \tag{2.51}$$

These are a set of Leggett-Garg inequalities.

2.2.3 Violation of Leggett-Garg Inequalities by Neutrinos

Neutrinos provide a good testing ground for LGIs since they have long range coherence (as they do not interact much with matter). Violations of LGIs by neutrinos have been measured experimentally.

Here I will first define the dichotomous variable for neutrinos propagating in accordance with the model shown in 1 and calculate the two time correlation function using that model. I will then calculate the Leggett-Garg parameters K_3 and K_4 for this system and plot the values to show how this system violates the LGIs, reproducing some of the results of [10].

For quantum systems, it can be shown [11] that

$$C_{ij} = \frac{1}{2} \langle \psi_i | \{\hat{Q}(t_i), \hat{Q}(t_j)\} | \psi_i \rangle . \tag{2.52}$$

Where $\hat{Q}(t_i)$ is the dichotomous observable which has been promoted to an operator $\hat{Q}$ in the Heisenberg picture.

Consider two flavour Neutrino oscillations wherein we have NIM.

Defining the dichotomous variable to be:

+1 when the system is in the state $|\nu_e(t_1)\rangle$ (i.e. $\langle \nu_e(t_1)|\psi(t)\rangle = 1$)

-1 when the system is in the state $|\nu_\mu(t_1)\rangle$ (i.e. $\langle \nu_\mu(t_1)|\psi(t)\rangle = 1$)

Calculation of C_{ij}

In order to calculate C_{12}, we need to know the probability distribution function, $\mathbf{P}(s_1, s_2)$. (This is the marginal probability distribution which can be obtained from the joint probability distribution by summing out Q_3).

Say that the initial state of the system is $|\nu_\mu\rangle$. $\mathbf{P}(Q_1 = -1, Q_2 = 1)$ corresponds to the probability of finding the particle to be in the state $|\nu_\mu\rangle$ at time t_1 and in the state $|\nu_e\rangle$ at time t_2. Due to the NIM assumption, the wave-function would not collapse when we make a measurement at time t_1.

Defining $\tau = t_2 - t_1$.

This probability would be the product of transition probability from $\nu_\mu \to \nu_\mu$ in time t_1 and the transition probability from $\nu_\mu \to \nu_e$ in time $\tau = t_2 - t_2$.

In general,

$$\mathbf{P}(\nu_\alpha, \nu_\beta) = \mathcal{P}_{\mu\to\alpha}(t_1)\mathcal{P}_{\alpha\to\beta}(\tau). \tag{2.53}$$

Here, it is understood that ν_μ corresponds to -1 and ν_e corresponds to 1, as per our definition of the dichotomous variable.

Substituting (2.53) in (2.43), we can calculate C_{12} as,

$$\begin{aligned} C_{12} =& \mathcal{P}_{\mu\to e}(t_1)\mathcal{P}_{e\to e}(\tau) - \mathcal{P}_{\mu\to e}(t_1)\mathcal{P}_{e\to\mu}(\tau) + \\ & - \mathcal{P}_{\mu\to\mu}(t_1)\mathcal{P}_{\mu\to e}(\tau) + \mathcal{P}_{\mu\to\mu}(t_1)\mathcal{P}_{\mu\to\mu}(\tau). \end{aligned} \tag{2.54}$$

Now we substitute (1.18) and (1.17) above. $\Delta m^2 := \Delta m^2_{12}$

$$
\begin{aligned}
C_{12} = &\sin^2 2\theta \sin^2\left(\frac{\Delta m^2 t_1}{4|\mathbf{p}|}\right)\left[1-\sin^2 2\theta \sin^2\left(\frac{\Delta m^2 \tau}{4|\mathbf{p}|}\right)\right] - \sin^2 2\theta \sin^2\left(\frac{\Delta m^2 t_1}{4|\mathbf{p}|}\right)\sin^2 2\theta \sin^2\left(\frac{\Delta m^2 \tau}{4|\mathbf{p}|}\right) \\
&- \left[1-\sin^2 2\theta \sin^2\left(\frac{\Delta m^2 t_1}{4|\mathbf{p}|}\right)\right]\sin^2 2\theta \sin^2\left(\frac{\Delta m^2 \tau}{4|\mathbf{p}|}\right) + \left(\left[1-\sin^2 2\theta \sin^2\left(\frac{\Delta m^2 t_1}{4|\mathbf{p}|}\right)\right]\right. \\
&\left.\times\left[1-\sin^2 2\theta \sin^2\left(\frac{\Delta m^2 \tau}{4|\mathbf{p}|}\right)\right]\right).
\end{aligned}
\tag{2.55}
$$

Expanding the products and simplifying we get:

$$
C_{12} = 1 - 2\sin^2 2\theta \sin^2\left(\frac{\Delta m^2 \tau}{4p}\right). \tag{2.56}
$$

Similarly one can show that if $t_2 - t_1 = t_3 - t_2 = \tau$, then

$$
C_{12} = C_{23} = C_{31} = 1 - 2\sin^2 2\theta \sin^2\left(\frac{\Delta m^2 \tau}{4p}\right). \tag{2.57}
$$

Calculation of K_3 and K_4

Now substituting this in (2.46) to get K_3, and in (2.50) with $n = 4$ to get K_4 we obtain :

$$
\begin{aligned}
K_3 &= 1 - 2\sin^2 2\theta \left[2\sin^2\frac{\Delta m^2 \tau}{4E} - \sin^2\frac{2\Delta m^2 \tau}{4E}\right], \\
K_4 &= 2 - 2\sin^2 2\theta \left[3\sin^2\frac{\Delta m^2 \tau}{4E} - \sin^2\frac{3\Delta m^2 \tau}{4E}\right].
\end{aligned}
\tag{2.58}
$$

Plotting K_3 and K_4

I then replicated the plots of [10] for K_3 and K_4.

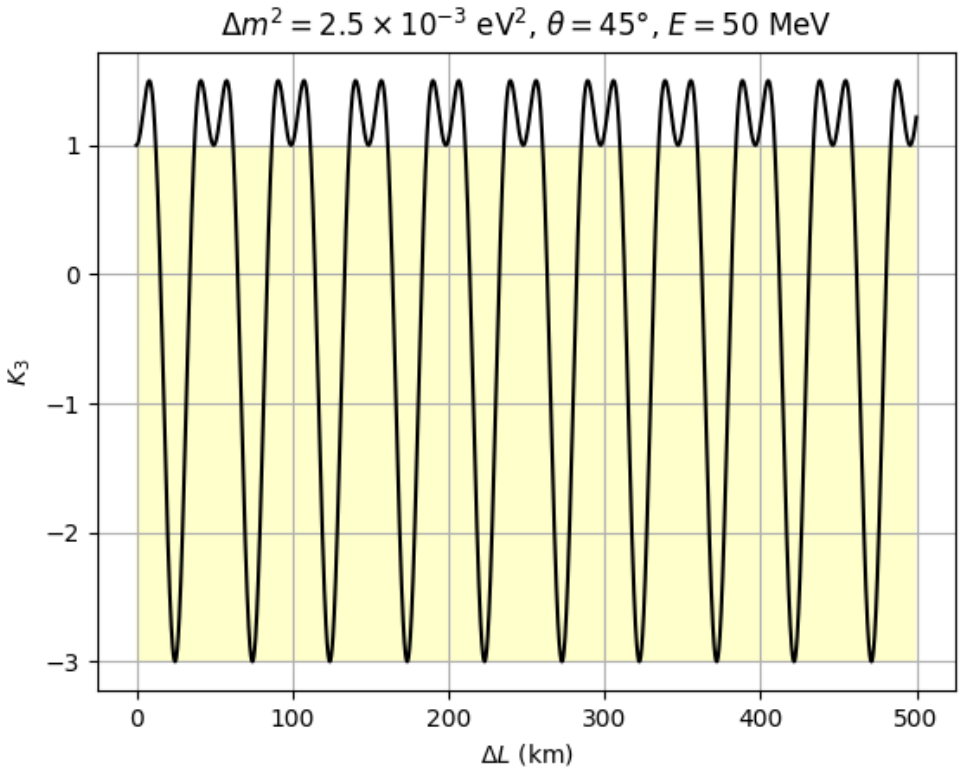

Figure 5 Plot of K_3. $\Delta L = c\tau$ and $E \approx p$ since neutrinos travell at ultra-relativistic speeds. The yellow shaded region is the region bounded by the classical inequality. Note that the violation of the inequality goes up to 3/2.

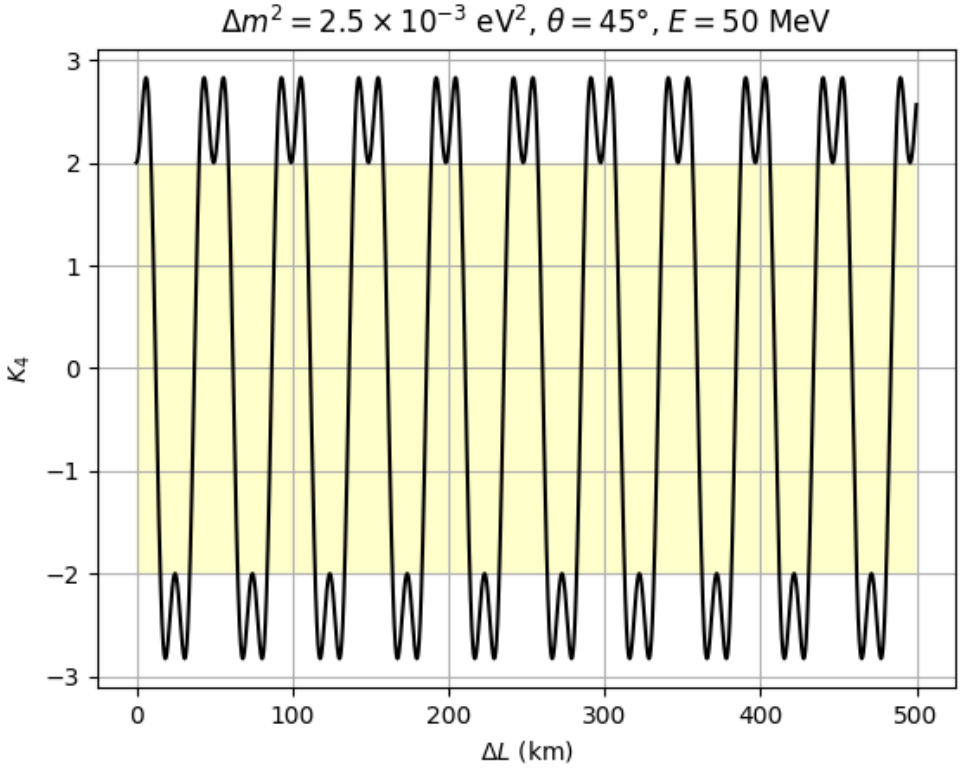

Figure 6 Plot of K_4. $\Delta L = c\tau$ and $E \approx p$ since neutrinos travell at ultra-relativistic speeds. The yellow shaded region is the region bounded by the classical inequality.

As can be seen above, our system violates the upper bound for K_3 and the upper and the lower bound for K_4.

Chapter 3

Results

After having used the technique developed in [4] to calculate the following 16 oscillation probabilities,

$$\nu_{e(\mu)}^{L(R)} \rightarrow \begin{cases} \nu_e^L \\ \nu_e^R \\ \nu_\mu^L \\ \nu_\mu^R \end{cases}$$

I used those transition probabilities to calculate the two time correlation function C_{ij} for relativistic neutrinos in magnetic fields. I will outline my calculations and the results.

I defined the dichotomous variable here to be the same as the one that we took in the no magnetic field case:

$+1$ when the system is in the state $|\nu_e^L\rangle$ or $|\nu_e^R\rangle$
(i.e. $\langle\nu_e^L|\psi(t)\rangle = 1$ or $\langle\nu_e^R|\psi(t)\rangle = 1$)

$+1$ when the system is in the state $|\nu_\mu^L\rangle$ or $|\nu_\mu^R\rangle$
(i.e. $\langle\nu_\mu^L|\psi(t)\rangle = 1$ or $\langle\nu_\mu^R|\psi(t)\rangle = 1$)

Where the state of the system if given by $|\psi(t)\rangle$ at time t.

3.1 Calculation of C_{ij} and K_3

Since there are two orthogonal states corresponding to the same value of the dichotomous variable, while calculating the joint probability distribution function $\mathbf{P}(s_1, s_2)$ we will have sum over all the $2 \times 2 = 4$ helicity states which introduce a degeneracy in the values of Q as shown:

I have taken the initial condition to be $|\nu_e^L\rangle$ and $\tau = t_2 - t_1$.

$$\begin{aligned}\mathbf{P}(Q_1 = 1, Q_2 = 1) =& \mathcal{P}_{\nu_e^L \rightarrow \nu_e^L}(t_1)\mathcal{P}_{\nu_e^L \rightarrow \nu_e^L}(\tau) + \mathcal{P}_{\nu_e^L \rightarrow \nu_e^L}(t_1)\mathcal{P}_{\nu_e^L \rightarrow \nu_e^R}(\tau) + \\ & \mathcal{P}_{\nu_e^L \rightarrow \nu_e^R}(t_1)\mathcal{P}_{\nu_e^R \rightarrow \nu_e^L}(\tau) + \mathcal{P}_{\nu_e^L \rightarrow \nu_e^R}(t_1)\mathcal{P}_{\nu_e^R \rightarrow \nu_e^R}(\tau).\end{aligned} \tag{3.1}$$

$$\begin{aligned}\mathbf{P}(Q_1 = 1, Q_2 = -1) =& \mathcal{P}_{\nu_e^L \rightarrow \nu_e^L}(t_1)\mathcal{P}_{\nu_e^L \rightarrow \nu_\mu^L}(\tau) + \mathcal{P}_{\nu_e^L \rightarrow \nu_e^L}(t_1)\mathcal{P}_{\nu_e^L \rightarrow \nu_\mu^R}(\tau) + \\ & \mathcal{P}_{\nu_e^L \rightarrow \nu_e^R}(t_1)\mathcal{P}_{\nu_e^R \rightarrow \nu_\mu^L}(\tau) + \mathcal{P}_{\nu_e^L \rightarrow \nu_e^R}(t_1)\mathcal{P}_{\nu_e^R \rightarrow \nu_\mu^R}(\tau).\end{aligned} \tag{3.2}$$

$$\begin{aligned}\mathbf{P}(Q_1 = -1, Q_2 = 1) =& \mathcal{P}_{\nu_e^L \rightarrow \nu_\mu^L}(t_1)\mathcal{P}_{\nu_\mu^L \rightarrow \nu_e^L}(\tau) + \mathcal{P}_{\nu_e^L \rightarrow \nu_\mu^L}(t_1)\mathcal{P}_{\nu_\mu^L \rightarrow \nu_e^R}(\tau) + \\ & \mathcal{P}_{\nu_e^L \rightarrow \nu_\mu^R}(t_1)\mathcal{P}_{\nu_\mu^R \rightarrow \nu_e^L}(\tau) + \mathcal{P}_{\nu_e^L \rightarrow \nu_\mu^R}(t_1)\mathcal{P}_{\nu_\mu^R \rightarrow \nu_e^R}(\tau).\end{aligned} \tag{3.3}$$

$$\begin{aligned}\mathbf{P}(Q_1=-1,Q_2=-1) =& \mathcal{P}_{\nu_e^L\to\nu_\mu^L}(t_1)\mathcal{P}_{\nu_\mu^L\to\nu_\mu^L}(\tau)+\mathcal{P}_{\nu_e^L\to\nu_\mu^L}(t_1)\mathcal{P}_{\nu_\mu^L\to\nu_\mu^R}(\tau)+\\ & \mathcal{P}_{\nu_e^L\to\nu_\mu^R}(t_1)\mathcal{P}_{\nu_\mu^R\to\nu_\mu^L}(\tau)+\mathcal{P}_{\nu_e^L\to\nu_\mu^R}(t_1)\mathcal{P}_{\nu_\mu^R\to\nu_\mu^R}(\tau).\end{aligned} \tag{3.4}$$

Substituting these in (2.43) (after having summed out the Q_3 random variable to obtain the marginal distribution), in addition to the transition amplitudes in A, I obtained after a laborious calculation:

$$\begin{aligned}C_{12} &= \sum_{s_1,s_2=\pm1} s_1 s_2 \mathbf{P}(Q_1=s_1,Q_2=s_2)\\ &= \cos^2 2\theta + \sin^2 2\theta \cos(2B_\perp \mu_- \tau)\cos^2\left(\frac{\Delta m^2 \tau}{2p}\right).\end{aligned} \tag{3.5}$$

Additionally assuming $t_2 - t_1 = t_3 - t_2 = \tau$ we get

$$\boxed{C_{ij} = \cos^2 2\theta + \sin^2 2\theta \cos(2B_\perp \mu_- \tau)\cos^2\left(\frac{\Delta m^2 \tau}{2p}\right).}$$

Where

$$\mu_- = \frac{\mu_1 - \mu_2}{2}.$$

Note that C_{ij} depends on $B_\perp$ only through μ_-, so if $\mu_1 = \mu_2$ or if $B_\perp = 0$, we happen to arrive at the same C_{ij} as in (2.56).

Now we can substitute the above form of C_{ij} into (2.50) for $n = 3$ and obtain

$$\boxed{K_3 = \cos^2 2\theta + 2\cos(2B_\perp \mu_- \tau)\cos\left(\frac{\Delta m^2 \tau}{2p}\right)\sin^2 2\theta - \cos(2B_\perp \mu_- \tau)\cos\left(\frac{\Delta m^2 \tau}{p}\right).}$$

3.2 Plotting K_3

Some plots of K_3 with varying magnetic fields are shown below in the high energy, small magnetic moment limit.

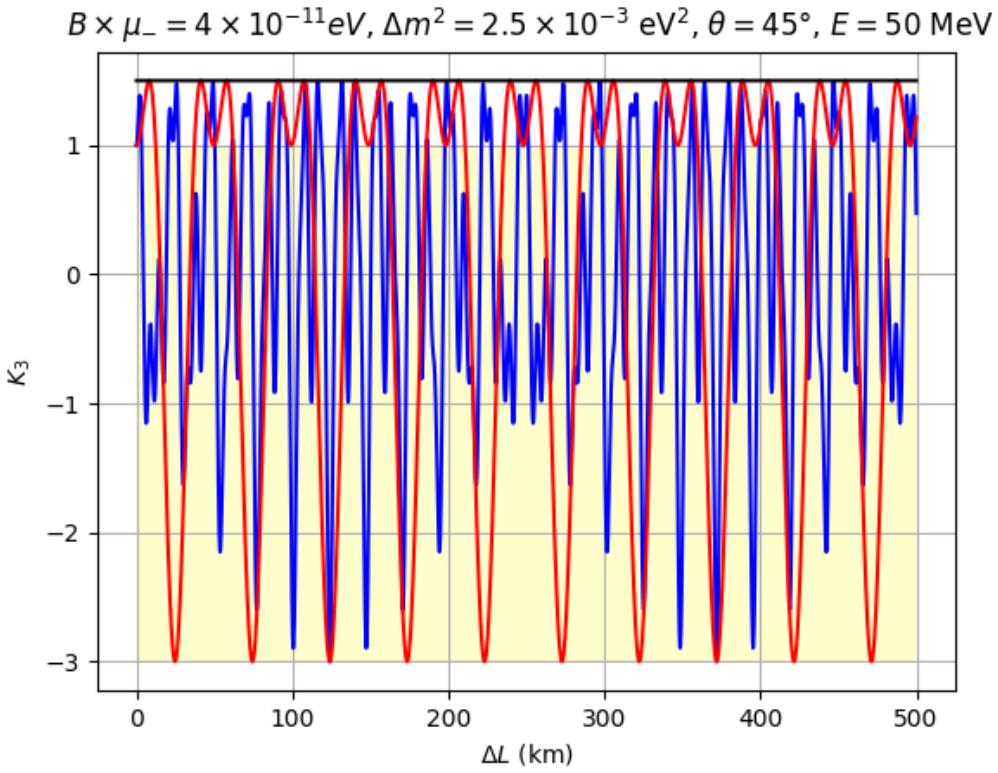

Figure 1 Plot of K_3. $\Delta L = c\tau$ and $E \approx p$ since neutrinos travell at ultra-relativistic speeds. The yellow shaded region is the region bounded by the classical inequality.The red line if for $B\mu_- = 0$, and the blue line is for $B\mu_- \neq 0$

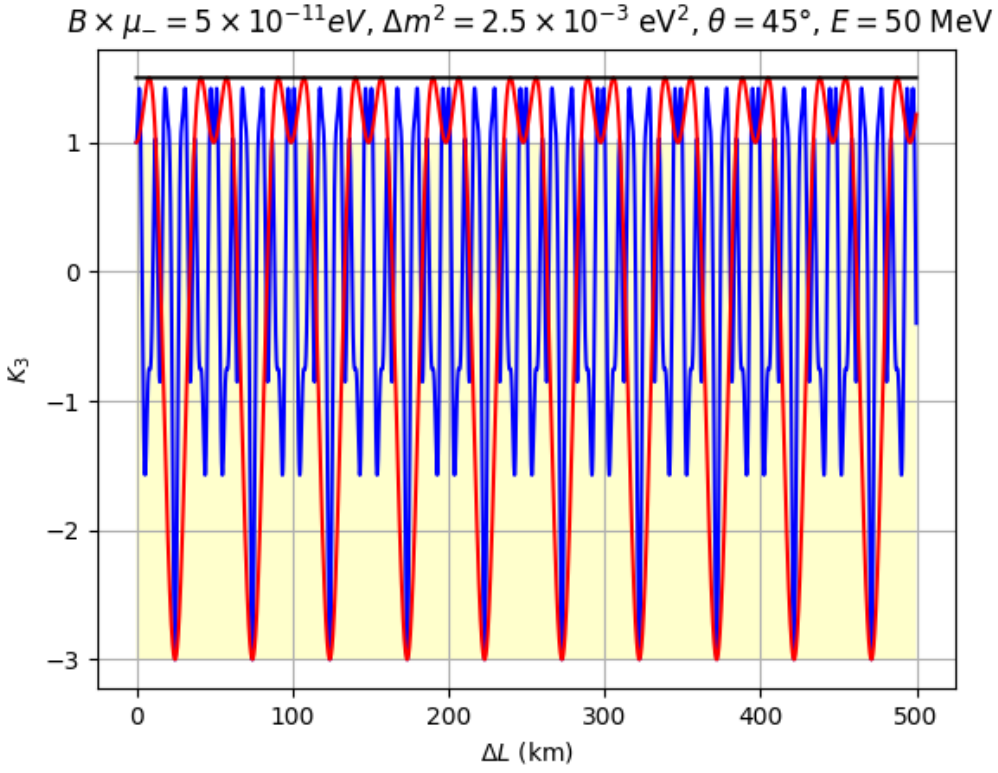

Figure 2 Plot of K_3. $\Delta L = c\tau$ and $E \approx p$ since neutrinos travell at ultra-relativistic speeds. The yellow shaded region is the region bounded by the classical inequality.The red line if for $B\mu_- = 0$, and the blue line is for $B\mu_- \neq 0$

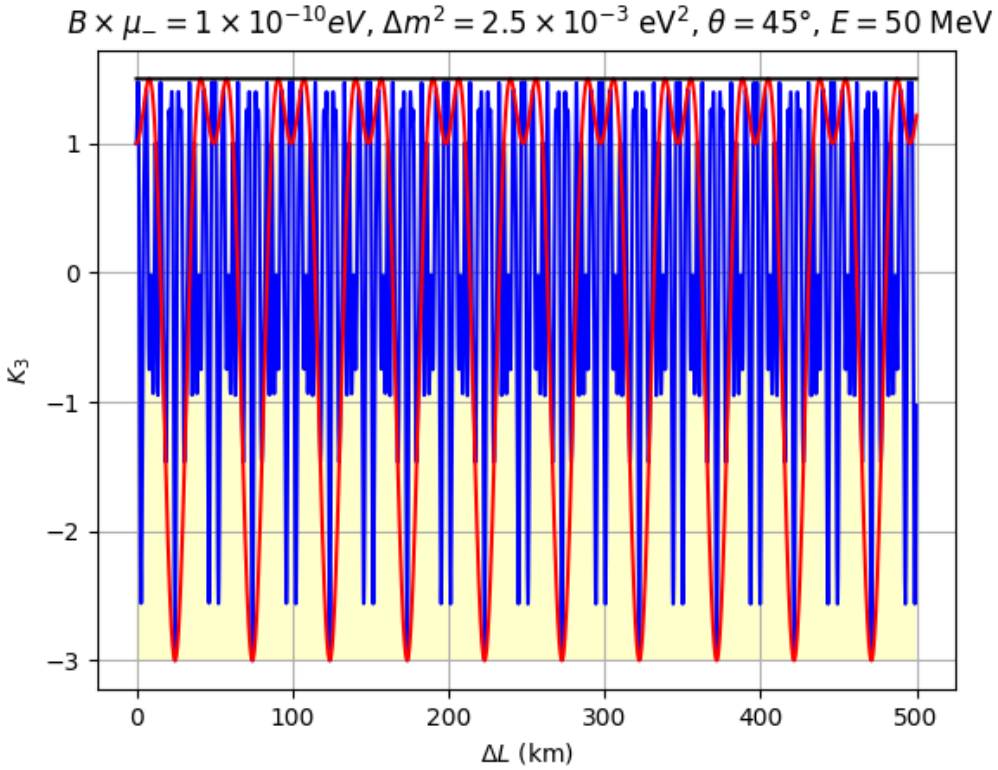

Figure 3 Plot of K_3. $\Delta L = c\tau$ and $E \approx p$ since neutrinos travell at ultra-relativistic speeds. The yellow shaded region is the region bounded by the classical inequality.The red line if for $B\mu_- = 0$, and the blue line is for $B\mu_- \neq 0$

The black line on top is the $K_3 = 3/2$ line. We note that K_3 does not exceed that line even if we have a non-zero magnetic field. We observe that as $B_\perp$ increases, the frequency of K_3 also increases.

Chapter 4

Conclusion and Future Discussions

After having used the techniques developed in [4] to reproduce their results for the four ν_e^L transition probabilities and using those techniques to calculate the rest twelve transition probabilities, I extended and applied the formalism for studying LGIs through the lens of neutrino oscillations to the case of neutrinos with non-zero spin in the presence of a magnetic field.

I successfully obtained the two time correlation function C_{ij} for this case, and used it to find the Leggett-Garg parameter K_3.

I found that the maximum violations of the LGI for K_3 is the same for the the treatment in which we include spin and have a non zero magnetic field and the treatment in which there is no spin.

This is slightly puzzling since there are a greater number of orthogonal states corresponding to the same value of the dichotomous variable[1] which would cause one to expect a greater violation of the LGIs [9].

It would be interesting to look into bounds for how great a violation can be for Leggett-Garg inequalities for quantum systems, (if such a bound exists, like Tsirelson's bound for the CHSH inequality), and if it is possible to achieve that bounds using a system comprising of neutrinos. One could also look into trying to construct new dichotomous variables for this system and see the violations of LGIs for that variable.

[1] for the treatment in which we include spin and have a non zero magnetic field compared to the no spin and no magnetic field case

Appendix A

Oscillation Probabilities in a Magnetic Field

Here I will show the results of my brute force calculations for the following transition amplitudes for completeness:

$$\nu_{e(\mu)}^{L(R)} \to \begin{cases} \nu_e^L \\ \nu_e^R \\ \nu_\mu^L \\ \nu_\mu^R \end{cases}$$

A.1 ν_e^L Transition Probabilities

A.1.1 Flavour Oscillation $\nu_e^L \to \nu_\mu^L$

$$\begin{aligned} \mathcal{P}_{\nu_e^L \to \nu_\mu^L}(t) = \sin^2 2\theta \Big[& \sin^2(\mu_+ B_\perp t) \sin^2(\mu_- B_\perp t) \\ & + \cos(\mu_2 B_\perp t) \cos(\mu_1 B_\perp t) \sin^2\left(\frac{\Delta m^2 t}{4p}\right)\Big]. \end{aligned} \tag{A.1}$$

A.1.2 Helicity Oscillation $\nu_e^L \to \nu_e^R$

$$\begin{aligned} \mathcal{P}_{\nu_e^L \to \nu_e^R}(t) &= |\, \langle \nu_e^R(0) | \nu_e^L(t) \rangle \,|^2, \\ \mathcal{P}_{\nu_e^L \to \nu_e^R}(t) &= \Big\{ \sin(\mu_+ B_\perp t) \cos(\mu_- B_\perp t) + \cos 2\theta \sin(\mu_- B_\perp t) \cos(\mu_+ B_\perp t) \Big\}^2 \\ &\quad - \sin^2 2\theta \sin(\mu_1 B_\perp t) \sin(\mu_2 B_\perp t) \sin^2\left(\frac{\Delta m^2}{4p} t\right). \end{aligned} \tag{A.2}$$

A.1.3 Helicity and Flavour Oscillation $\nu_e^L \to \nu_\mu^R$

$$\begin{aligned} \mathcal{P}_{\nu_e^L \to \nu_\mu^R}(t) &= |\, \langle \nu_\mu^R(0) | \nu_e^L(t) \rangle \,|^2, \\ \mathcal{P}_{\nu_e^L \to \nu_\mu^R}(t) &= \sin^2 2\theta \Big\{ \sin^2(\mu_- B_\perp t) \cos^2(\mu_+ B_\perp t) + \sin(\mu_1 B_\perp t) \sin(\mu_2 B_\perp t) \sin^2 \frac{\Delta m^2}{4p} t \Big\}. \end{aligned} \tag{A.3}$$

A.1.4 Survival Probability $\nu_e^L \to \nu_e^L$

$$\begin{aligned}\mathcal{P}_{\nu_e^L\to\nu_e^L}(t) &= |\,\langle\nu_e^L(0)|\nu_e^L(t)\rangle\,|^2,\\ \mathcal{P}_{\nu_e^L\to\nu_e^L}(t) &= \Big\{\cos(\mu_+B_\perp t)\cos(\mu_-B_\perp t) - \cos 2\theta\sin(\mu_+B_\perp t)\sin(\mu_-B_\perp t)\Big\}^2\\ &\quad - \sin^2 2\theta\cos(\mu_1B_\perp t)\cos(\mu_2B_\perp t)\sin^2\left(\frac{\Delta m^2}{4p}t\right).\end{aligned} \tag{A.4}$$

A.2 ν_e^R Transition Probabilities

A.2.1 Flavour Oscillation $\nu_e^R \to \nu_\mu^R$

$$\begin{aligned}\mathcal{P}_{\nu_e^L\to\nu_\mu^L}(t) = \sin^2 2\theta\Big[&\sin^2(\mu_+B_\perp t)\sin^2(\mu_-B_\perp t),\\ &+\cos(\mu_2B_\perp t)\cos(\mu_1B_\perp t)\sin^2\left(\frac{\Delta m^2 t}{4p}\right)\Big].\end{aligned} \tag{A.5}$$

A.2.2 Helicity Oscillation $\nu_e^R \to \nu_e^L$

$$\begin{aligned}\mathcal{P}_{\nu_e^R\to\nu_e^L}(t) &= \Big\{\sin(\mu_+B_\perp t)\cos(\mu_-B_\perp t) + \cos 2\theta\sin(\mu_-B_\perp t)\cos(\mu_+B_\perp t)\Big\}^2\\ &\quad - \sin^2 2\theta\sin(\mu_1B_\perp t)\sin(\mu_2B_\perp t)\sin^2\left(\frac{\Delta m^2}{4p}t\right).\end{aligned} \tag{A.6}$$

A.2.3 Helicity and Flavour Oscillation $\nu_e^R \to \nu_\mu^L$

$$\mathcal{P}_{\nu_e^R\to\nu_\mu^L}(t) = \sin^2 2\theta\Big\{\sin^2(\mu_-B_\perp t)\cos^2(\mu_+B_\perp t) + \sin(\mu_1B_\perp t)\sin(\mu_2B_\perp t)\sin^2\frac{\Delta m^2}{4p}t\Big\}. \tag{A.7}$$

A.2.4 Survival Probability $\nu_e^R \to \nu_e^R$

$$\begin{aligned}\mathcal{P}_{\nu_e^R\to\nu_e^R}(t) &= \Big\{\cos(\mu_+B_\perp t)\cos(\mu_-B_\perp t) - \cos 2\theta\sin(\mu_+B_\perp t)\sin(\mu_-B_\perp t)\Big\}^2\\ &\quad - \sin^2 2\theta\cos(\mu_1B_\perp t)\cos(\mu_2B_\perp t)\sin^2\left(\frac{\Delta m^2}{4p}t\right).\end{aligned} \tag{A.8}$$

A.3 ν_μ^L Transition Probabilities

A.3.1 Flavour Oscillation $\nu_\mu^L \to \nu_e^L$

$$\begin{aligned}\mathcal{P}_{\nu_\mu^L\to\nu_e^L}(t) = \sin^2 2\theta\Big[&\sin^2(\mu_+B_\perp t)\sin^2(\mu_-B_\perp t)\\ &+\cos(\mu_2B_\perp t)\cos(\mu_1B_\perp t)\sin^2\left(\frac{\Delta m^2 t}{4p}\right)\Big].\end{aligned} \tag{A.9}$$

A.3.2 Helicity Oscillation $\nu_\mu^L \to \nu_\mu^R$

$$\begin{aligned}\mathcal{P}_{\nu_\mu^L\to\nu_\mu^R}(t) &= \Big\{\sin(\mu_+B_\perp t)\cos(\mu_-B_\perp t) - \cos 2\theta\sin(\mu_-B_\perp t)\cos(\mu_+B_\perp t)\Big\}^2\\ &\quad - \sin^2 2\theta\sin(\mu_1B_\perp t)\sin(\mu_2B_\perp t)\sin^2\left(\frac{\Delta m^2}{4p}t\right).\end{aligned} \tag{A.10}$$

A.3.3 Helicity and Flavour Oscillation $\nu_\mu^L \to \nu_e^R$

$$\mathcal{P}_{\nu_\mu^L \to \nu_e^R}(t) = \sin^2 2\theta \Big\{ \sin^2(\mu_- B_\perp t) \cos^2(\mu_+ B_\perp t) + \sin(\mu_1 B_\perp t) \sin(\mu_2 B_\perp t) \sin^2 \frac{\Delta m^2}{4p} t \Big\}. \tag{A.11}$$

A.3.4 Survival Probability $\nu_\mu^L \to \nu_\mu^L$

$$\begin{aligned} \mathcal{P}_{\nu_\mu^L \to \nu_\mu^L}(t) = & \Big\{ \cos(\mu_+ B_\perp t) \cos(\mu_- B_\perp t) + \cos 2\theta \sin(\mu_+ B_\perp t) \sin(\mu_- B_\perp t) \Big\}^2 \\ & - \sin^2 2\theta \cos(\mu_1 B_\perp t) \cos(\mu_2 B_\perp t) \sin^2 \left(\frac{\Delta m^2}{4p} t \right). \end{aligned} \tag{A.12}$$

A.4 ν_μ^R Transition Probabilities

A.4.1 Flavour Oscillation $\nu_\mu^R \to \nu_e^R$

$$\begin{aligned} \mathcal{P}_{\nu_\mu^R \to \nu_\mu^R}(t) = \sin^2 2\theta \Big[& \sin^2(\mu_+ B_\perp t) \sin^2(\mu_- B_\perp t) \\ & + \cos(\mu_2 B_\perp t) \cos(\mu_1 B_\perp t) \sin^2 \left(\frac{\Delta m^2 t}{4p} \right) \Big]. \end{aligned} \tag{A.13}$$

A.4.2 Helicity Oscillation $\nu_\mu^R \to \nu_\mu^L$

$$\begin{aligned} \mathcal{P}_{\nu_\mu^R \to \nu_\mu^L}(t) = & \Big\{ \sin(\mu_+ B_\perp t) \cos(\mu_- B_\perp t) - \cos 2\theta \sin(\mu_- B_\perp t) \cos(\mu_+ B_\perp t) \Big\}^2 \\ & - \sin^2 2\theta \sin(\mu_1 B_\perp t) \sin(\mu_2 B_\perp t) \sin^2 \left(\frac{\Delta m^2}{4p} t \right). \end{aligned} \tag{A.14}$$

A.4.3 Helicity and Flavour Oscillation $\nu_\mu^R \to \nu_e^L$

$$\mathcal{P}_{\nu_\mu^R \to \nu_e^L}(t) = \sin^2 2\theta \Big\{ \sin^2(\mu_- B_\perp t) \cos^2(\mu_+ B_\perp t) + \sin(\mu_1 B_\perp t) \sin(\mu_2 B_\perp t) \sin^2 \frac{\Delta m^2}{4p} t \Big\}. \tag{A.15}$$

A.4.4 Survival Probability $\nu_\mu^R \to \nu_\mu^R$

$$\begin{aligned} \mathcal{P}_{\nu_\mu^R \to \nu_\mu^R}(t) = & \Big\{ \cos(\mu_+ B_\perp t) \cos(\mu_- B_\perp t) + \cos 2\theta \sin(\mu_+ B_\perp t) \sin(\mu_- B_\perp t) \Big\}^2 \\ & - \sin^2 2\theta \cos(\mu_1 B_\perp t) \cos(\mu_2 B_\perp t) \sin^2 \left(\frac{\Delta m^2}{4p} t \right). \end{aligned} \tag{A.16}$$

Bibliography

[1] David J. Griffiths. *Introduction to Elementary Particles, 2nd, Revised Edition*, pages 387–397. John Wiley & Sons, 2008.

[2] Mark Thomson. *Modern Particle Physics*, pages 329–360. Cambridge University Press, 2013.

[3] E. Kh. Akhmedov and A. Yu. Smirnov. Paradoxes of neutrino oscillations. *Physics of Atomic Nuclei*, 72(8):1363–1381, August 2009.

[4] Artem Popov and Alexander Studenikin. Neutrino eigenstates and flavour, spin and spin-flavour oscillations in a constant magnetic field. *The European Physical Journal C*, 79(2), February 2019.

[5] M.E. Peskin and D.V. Schroeder. *An Introduction to Quantum Field Theory*. CRC Press, 1995.

[6] Chinhsan Sieng. Neutrino Oscillations in the Presence of a Magnetic Field. *Macalester Journal of Physics and Astronomy*, 10, May 2022.

[7] Michael A. Nielsen and Isaac L. Chuang. *Quantum Computation and Quantum Information: 10th Anniversary Edition*, page 111. Cambridge University Press, 2010.

[8] A. J. Leggett and Anupam Garg. Quantum mechanics versus macroscopic realism: Is the flux there when nobody looks? *Phys. Rev. Lett.*, 54:857–860, Mar 1985.

[9] Clive Emary, Neill Lambert, and Franco Nori. Leggett–Garg inequalities. *Reports on Progress in Physics*, 77(1):016001, December 2013.

[10] Bhavya Soni, Sheeba Shafaq, and Poonam Mehta. Distinguishing between Dirac and Majorana neutrinos using temporal correlations, 2023.

[11] Tobias Fritz. Quantum correlations in the temporal Clauser–Horne–Shimony–Holt (CHSH) scenario. *New Journal of Physics*, 12(8):083055, August 2010.